A membrane-associated thioredoxin required for plant growth moves from cell to cell, suggestive of a role in intercellular communication

Ling Meng, Joshua H. Wong, Lewis J. Feldman, Peggy G. Lemaux, and Bob B. Buchanan[1]

Department of Plant and Microbial Biology, University of California, Berkeley, CA 94720

Contributed by Bob B. Buchanan, December 1, 2009 (sent for review September 24, 2009)

Thioredoxins (Trxs) are small ubiquitous regulatory disulfide proteins. Plants have an unusually complex complement of Trxs composed of six well-defined types (Trxs *f*, *m*, *x*, *y*, *h*, and *o*) that reside in different cell compartments and function in an array of processes. The extraplastidic *h* type consists of multiple members that in general have resisted isolation of a specific phenotype. In analyzing mutant lines in *Arabidopsis thaliana*, we identified a phenotype of dwarf plants with short roots and small yellowish leaves for AtTrx *h*9 (henceforth, Trx *h*9), a member of the *Arabidopsis* Trx *h* family. Trx *h*9 was found to be associated with the plasma membrane and to move from cell to cell. Controls conducted in conjunction with the localization of Trx *h*9 uncovered another *h*-type Trx in mitochondria (Trx *h*2) and a Trx in plastids earlier described as a cytosolic form in tomato. Analysis of Trx *h*9 revealed a 17-amino acid N-terminal extension in which the second Gly (Gly^2) and fourth cysteine (Cys^4) were highly conserved. Mutagenesis experiments demonstrated that Gly^2 was required for membrane binding, possibly via myristoylation. Both Gly^2 and Cys^4 were needed for movement, the latter seemingly for protein structure and palmitoylation. A three-dimensional model was consistent with these predictions as well as with earlier evidence showing that a poplar ortholog is reduced by a glutaredoxin rather than NADP-thioredoxin reductase. In demonstrating the membrane location and intercellular mobility of Trx *h*9, the present results extend the known boundaries of Trx and suggest a role in cell-to-cell communication.

protein movement | redox regulation | signal transduction | thioredoxin *h* | myristoylation–palmitoylation

Current evidence indicates that redox state is one of the factors determining the fate and growth of cells during the development of multicellular organisms. The ubiquitous disulfide regulatory protein thioredoxin (Trx) appears to play a role in linking redox to this process (1, 2). Trxs belong to a complex family of regulatory proteins consisting of at least six distinct types in plants, *f*, *m*, *x*, *y*, *h*, and *o* (Fig. S1*A*). Trxs reside in different cell compartments and function in an array of processes. Whereas the role of chloroplast Trxs is relatively clear, our understanding of the function of the multiple members of the extraplastidic *h* type is limited. Moreover, mutant phenotypes of *h*-type Trxs are scant; a loss-of-function mutant has been described in only one case: Trx *h*5 was found to be required for response of *Arabidopsis* to fungal infection (3, 4).

In exploring the function of the *h* type of Trxs, we elected to focus on the member of this group whose ortholog, Trx *h*9, was recently found to be important in the germination of cereal seeds (5). As *Arabidopsis* appeared ideally suited for this purpose, we sought a phenotype for a mutant defective in this Trx. Our efforts have been successful: We now report the identification of a phenotype for a null, loss-of-function mutation in Trx *h*9. The *trx h*9 mutant, showed chlorotic leaves and impaired growth and development. In contrast to other Trxs tested as controls, Trx *h*9 was found to be associated with the plasma membrane and, surprisingly, was able to move from cell to cell. By constructing structural models, we found that *Arabidopsis* Trx *h*9 may be reduced with NADPH by glutaredoxin (Grx) and glutathione (GSH) rather than the usual NADP-thioredoxin reductase (NTR) enzyme as shown for its ortholog from poplar (6). Our findings suggest that Trx *h*9 plays a role in plant growth, possibly by allowing cells to relay redox information to one another.

Results and Discussion

***Arabidopsis* Trx *h*9.** Sequence analysis revealed that Trx *h*9 is evolutionarily conserved and shares high sequence identity with its orthologs in different species. For example, we found that 63% of the Trx *h*9 protein sequence is identical to that of its rice counterpart (Os01g0168200; GenBank accession no. NP_001042127), whereas only 46% is identical with Trx *h*1, the most closely related paralog in *Arabidopsis*. Based on an N-terminal extension characterized by a conserved Gly at position 2 (Gly^2) and a cysteine at position 4 (Cys^4), Trx *h*9 and its orthologs form a new branch of *h*-type Trxs clearly separate from other members of the group (Figs. S1 and S2*A*). These features suggest that this region may endow Trx *h*9 with unique functions and properties. The microarray data revealed that Trx *h*9 is expressed in a tissue-specific manner (Fig. S2*B*), although RT-PCR analyses showed that Trx *h*9 is expressed throughout the plant (Fig. S2*C*), consistent with results reported by Reichheld et al. (7). Expression was strongest in the epidermal cells in the elongation zone of the roots, stomata, stamen, and pollen (Fig. S2 *B* and *C* and Table S1).

Recessive Loss-of-Function Mutation in Trx *h*9 Impairs Growth and Development. Genetic screening of T-DNA insertions and subsequent sequencing revealed that Salk line 086660 contained a T-DNA insertion in the second exon of the *Trx h*9 coding sequence between the 135th and 136th nucleotide (Fig. S2*D*). RT-PCR results further indicated that homozygous Salk_086660 plants were null loss-of-function mutants of Trx *h*9 (Fig. S2*E*). There was no detectable *trx h*9 RNA in plants from two individual T_3 homozygous mutants of Salk_086660 (Salk_08660-3 and Salk_08660-9).

Phenotypic analyses revealed that loss of Trx *h*9 function seriously impaired growth and development. When cultured on Murashiga-Skoog (MS) medium without sucrose, mutant plants ceased growth after germination (Fig. S3*A*). Roots and leaves of the homozygous mutants were significantly shorter and smaller than wild-type counterparts grown on MS medium with 1% sucrose (Fig. 1 *A* and *B*). Root tips of 7-day-old mutant seedlings grown on MS medium with 1% sucrose had a shortened apical meristem and, cells were more compact, in keeping with noticeably shorter roots (Fig. 1*B*; Fig. S3*B*). When grown in soil, mutant plants were dwarf with small yellowish leaves (Fig. 1*C*; Fig. S3*C*).

Author contributions: L.M., P.G.L., and B.B.B. designed research; L.M., J.H.W., and L.J.F. performed research; L.M., P.G.L., and B.B.B. analyzed data; and L.M., L.J.F., P.G.L., and B.B.B. wrote the paper.

The authors declare no conflict of interest.

[1]To whom correspondence should be addressed. E-mail: view@berkeley.edu.

This article contains supporting information online at www.pnas.org/cgi/content/full/0913759107/DCSupplemental.

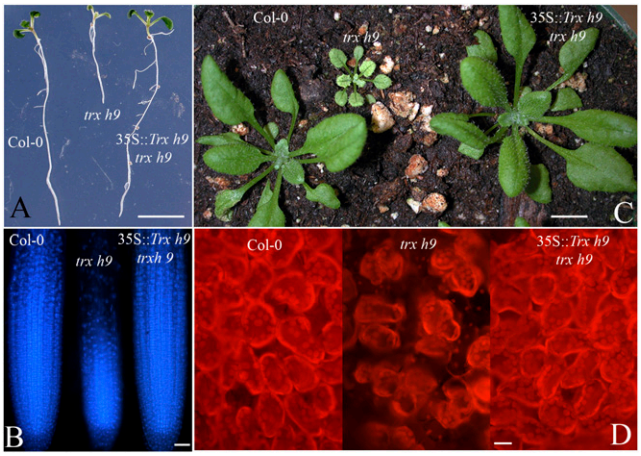

Fig. 1. Phenotypic and complementation analysis of *trx h*9 mutation in Salk_08660 plants. Seven-day-old *Arabidopsis* seedlings (*A*) and root tips (*B*) grown on MS medium plus 1.0% sucrose (left to right: wild-type *Arabidopsis* Col-0 plant, homozygous *trx h*9 mutant, and 35S::*Trx h*9 in *trx h*9 background). Root tips in *B* were fixed [methanol:acetic acid (3:1) buffer at 4°C overnight], stained with DAPI for 20 min, and viewed immediately under a fluorescence microscope. (*C*) Thirty-five-day-old *Arabidopsis* grown in soil. (*D*) Leaves from 35-day-old *Arabidopsis* grown in soil and viewed under a fluorescence microscope. Order in all panels is the same as (*A*). [Scale bars, 1 cm (*A* and *C*); 50 μm (*B* and *D*).]

Mesophyll cells from mutant leaves were smaller and irregularly shaped, with fewer chloroplasts versus wild type (Fig. 1*D*). Consistent with lower chloroplast numbers, mature rosette leaves of mutant plants contained on a relative basis ca 50% of the chlorophyll of wild type based on HPLC analysis (1477 vs. 760.7 for Chl a and 804.9 vs. 406.4 for Chl b in wild type and *ath*9 mutant, respectively). Heterozygous and F_1 plants from a backcross to Salk_086660 yielded a wild-type plant, suggesting that Salk_086660 contains a recessive Trx *h*9 mutation.

At this point, we deemed it desirable to characterize a novel *Arabidopsis* chloroplast Trx because the loss-of function Trx *h*9 seems to affect chloroplasts. For this purpose, we selected a previously unreported *Arabidopsis* Trx [called "putative thioredoxin" (GenBank accession no. NP_187329; TAIR: At3G06730) in the *Arabidopsis* Information Resource database] that was predicted to be in plastids based on the use of the ChloroP 1.1 Server (http://www.cbs.dtu.dk/services/ChloroP) and to be closely related to plastid Trx *y* (Fig. S1*A*). We provisionally designated this protein Trx*p*, due to its putative and plastidic nature. The Trx*p* ortholog in tomato, CITRX (Cf-9-interacting thioredoxin), was earlier shown to function in disease resistance (8). It was thus of interest to determine loss-of-function phenotypes of Trx *p* by studying a T-DNA insertion line, Salk_028162, in which a T-DNA was inserted at a position 161 bp upstream of the first intron of the *Trxp p* gene (Fig. S1*B*). This insertion resulted in a null knockout in the homozygous mutant plants (*trx p*) (Fig. S1*C*) which appeared completely albino, ceased growth, and died shortly after germination (Fig. S1*D*). Plastids in *trx p* plants lacked visible internal membrane structures, including stromal and granal thylakoids as well as starch granules (Fig. S1*F*). There were, however, many densely stained globular structures, possibly plastoglobuli of degenerated thylakoid lipids (9) (Fig. S1*G*). Trx *p* thus may play a role in plastid development in addition to its role in plant disease (8).

35S::Trx *h*9 Construct Fully Rescued the Loss-of-Function Phenotypes of Trx *h*9 Mutant. In further characterization of its function, the full-length Trx *h*9 gene driven by the 35S promoter was introduced into homozygous Salk_086660 mutant plants. Sixty individual transgenic 35S::*Trx h*9 lines in the *trx h*9 mutant background were analyzed in the T_1 generation. Complete rescue of the mutant phenotypes was observed in 44 lines (77.33%), yielding plants indistinguishable from wild-type *Arabidopsis* (Col-0) (Fig. 1 *A*–*D*). These results confirmed that the mutant phenotypes were due to the loss-of-function mutation in Trx *h*9.

Trx *h*9 Is a Plasma Membrane Protein. To obtain insight into its function, we determined the subcellular localization of Trx *h*9. We fused green fluorescence protein (GFP, a 27-kDa resident of the cytosol) in-frame to the full-length Trx *h*9 at the C terminus. Localization of the Trx *h*9-GFP fusion protein was assayed in both transient and stable transformation systems.

Before examining Trx *h*9, we tested GFP fusions with *Arabidopsis* proteins targeted to different organelles using the isolated onion epidermal cell layer for the transient expression assay. These studies revealed that free GFP (a cytosolic protein) was present throughout the cell (Fig. S4*A*). Moreover, when cells expressing free GFP were plasmolyzed, GFP remained in the cytosol (Fig. S4*B*), not in the Hechtian strands (see below) or cell wall, as revealed by DAPI staining (Fig. S4*C*). By contrast, when fused to a nuclear localization signal (NLS), GFP accumulated, as expected, in the nucleus (Fig. S4*D*). In short, GFP fused to control proteins was localized as predicted.

We also examined the location of Trx *p* that was predicted to be in plastids by the PSORT program (http://psort.ims.u-tokyo.ac.jp/form.html). Using transient and stable transformations with GFP fusions, we localized *Arabidopsis* Trx *p* in plastids (Fig. 2 *D* and *E*). In parallel transient expressions, the Trx *p* counterpart (GenBank accession no. BG299573) and Trx *f* (GenBank accession no. AK250725) from barley (*Hordeum vulgare*) were identically localized. This finding contrasts with the report that the Trx *p* ortholog from tomato, CITRX, is localized in the cytosol (8). Further work is needed to resolve this discrepancy.

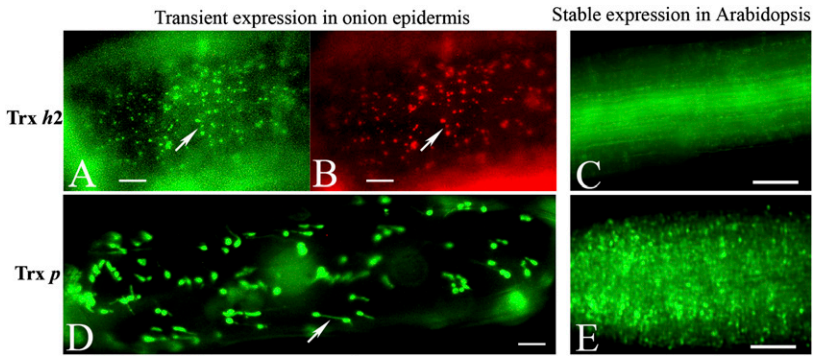

Fig. 2. Subcellular localization of Trx *h*2 and Trx *p* in onion epidermal and transgenic *Arabidopsis* cells using GFP tagging. (*A*–*C*) Trx *h*2 (At5g39950); (*D* and *E*) Trx *p* (At3G06730). (*A*, *B*, and *D*) Transient expression in onion epidermal cells. (*C* and *E*) Stable expression in transgenic *Arabidopsis* root cells. (*A*, *C*, *D*, and *E*) Visualization of GFP. (*B*) MitoTracker orange. [Scale bars, 10 μm (*A*, *B*, and *D*); 50 μm (*C* and *E*).] In *A* and *B*, arrows point to the same mitochondrion, and in *D* to the long stromule.

We also examined the localization of Trx *h*2, which, as anticipated, was in the cytosol. However, unexpectedly, it was also observed in mitochondria in the onion transient expression system. This location was seen with both the onion transient expression assay, where GFP (Fig. 2*A*) was colocalized using MitoTrack orange, a specific dye for mitochondria (Invitrogen) (Fig. 2*B*), and in stably transformed *Arabidopsis* (Fig. 2*C*). In addition to providing evidence for a mitochondrial *h*-type Trx in *Arabidopsis*, these results complement earlier work with castor seed (10) and poplar (11).

Cellular localization of Trx *h*9 was examined against this background. When transiently expressed in onion cells, Trx *h*9 fused to GFP localized to the cell periphery—that is, the plasma membrane, cell wall, or both (Fig. 3*A*). To localize the protein more accurately, onion cells were plasmolyzed after being transformed with Trx *h*9-GFP. Under these conditions, protoplasts pull away from the cell wall, becoming spherical and leaving large numbers of thin plasma membrane bridges, known as Hechtian strands, firmly anchored to the cell wall (12). Trx *h*9-GFP displayed a pattern consistent with its location in the plasma membrane (Fig. 3*B*, Hechtian strands marked with arrow). Similar results were obtained with the barley Trx *h*-like protein (GenBank accession no. AAN63616), an ortholog that shares 65% sequence identity with Trx *h*9.

Results obtained with Trx *h*9-GFP stably expressed in *Arabidopsis* were in agreement with the transient expression assays. GFP from Trx *h*9-GFP fusion proteins in transgenic *Arabidopsis* seedlings was observed in the plasma membrane and/or cell wall of root cells (Fig. 3*C*). Analyses of protoplasts from plants stably expressing Trx *h*9-GFP revealed that fluorescence remained in the plasma membrane of spherical protoplasts after cell walls were removed (Fig. 3*D*). Further, western blots using a GFP antibody demonstrated that the Trx *h*9-GFP fusion protein was prevalent in the insoluble, not the soluble, fraction extracted from transgenic plants stably expressing the protein (Fig. S5). This pattern contrasted with that of Trx *h*2, which localized to both the cytosol and mitochondria (Fig. 2 *A*–*C*). Overall, these results suggest that Trx *h*9 is a plasma membrane protein.

Trx *h*9 May Be Myristoylated and Palmitoylated. Although there are exceptions for mitochondria and endoplasmic reticulum, plant *h*-type Trxs are generally considered to be soluble, cytosolic proteins due to the absence of protein-sorting signals and transmembrane domains (10, 13, 14). However, other factors are known to affect membrane-binding properties of proteins through either co- or posttranslational addition of a variety of lipids, such as myristyl (C14), farnesyl (C15), palmityl (C16), and geranylgeranyl (C20) groups. Covalent linkage of these moieties to a protein can affect its membrane-binding properties (15). Trx *h*9 possesses a conserved N-terminal Gly (Gly^2) and Cys (Cys^4) suggestive of lipid modification. *N*-myristoylation refers to the cotranslational and irreversible addition of myristate at the N-terminal Gly of a protein via amide linkage (16, 17). Palmitoylation, on the other hand, represents a reversible posttranslational attachment of a palmityl group to specific Cys residues through thioester linkage (15, 18). Proteins with Cys residues adjacent to or near an *N*-myristoylated Gly residue, like Trx *h*9, may be sequentially palmitoylated (17).

By using a specific N-terminal prediction program, Myristoylator (http://ca.expasy.org/tools/myristoylator), we analyzed *Arabidopsis* Trxs for potential myristoylation. Trx *h*9 (At3g08710), Trx *h*2 (At5g39950), Trx *h*7 (At1G59730), and Trx *h*8 (At1G69880) were found to have high confidence scores for myristoylation (respective S values of 0.9872, 0.9864, 0.9890, and 0.9901). The S score is based on the average responses of 25 artificial neural network predictions, which are defined as S = positive minus negative; $0.85 < S < 1$ indicates a high confidence prediction. As the only *h*-type representative with the necessary third Cys (Cys^4) at the N terminus, Trx *h*9 was subjected to palmitoylation prediction using the CSS-PALM program (http://csspalm.biocuckoo.org). Perhaps not surprisingly, the N-terminal conserved Cys at position 4 (Cys^4) of Trx *h*9 was positive for palmitoylation with a score (S) of 4.852 ($S \geq 1.0$ indicates high confidence). Thus, whereas Trxs *h*2, *h*7, and *h*8 may be myristoylated, Trx *h*9 appears to be the only member of the Trx *h* group capable of undergoing dual lipid modification (myristoylation and palmitoylation). Furthermore, based on these analyses, we found that other plant Trxs (*f*, *m*, *x*, *y*, and *o*) would also not undergo lipid modification. The role of Gly (Gly^2) in Trxs *h*2, *h*7, and *h*8 is yet to be determined.

Mutation of Gly^2, Not Cys^4, in Conserved N-Terminal Extension Abolishes Trx *h*9 Membrane Localization. The Gly^2 and Cys^4 residues in the N-terminal extension of Trx *h*9 are highly conserved with its orthologs (Fig. S2*A*). Gly^2 and Cys^4 are canonical sites, respectively, for *N*-myristoylation and palmitoylation (15–17). Further, Cys^4 is required for catalysis of the poplar ortholog of Trx *h*9, PtTrxh4 (19). It was therefore of interest to determine the importance of Gly^2 and Cys^4 in Trx *h*9. To this end, the two amino acids were mutated to Ala^2 (Trx *h*9G2A) and Trp^4 (Trx *h*9C4W), respectively. Subcellular localization of the mutated GFP proteins was determined in both transient and stable transformants.

Mutation of Gly^2 abolished membrane localization, as seen with transient expression (Fig. 3*E*), such that Trx *h*9 showed typical cytosolic localization similar to GFP alone (Fig. S4*A*). Moreover, unlike Trx *h*9-GFP, Trx *h*9G2A-GFP fusion was not seen in the plasma membrane but rather was distributed in the cytosol, as visualized by GFP and confirmed by DAPI staining (Fig. 3*F*). In contrast to Gly^2, mutation of Cys^4 did not affect localization of Trx *h*9, which, like the wild type, was observed in the plasma membrane (Fig. 3 *I* and *J*). Results with stably transformed *Arabidopsis* were consistent with transient expression assays of the mutants in both Gly^2 (Fig. 3 *G* and *H*) and Cys^4 (Fig.

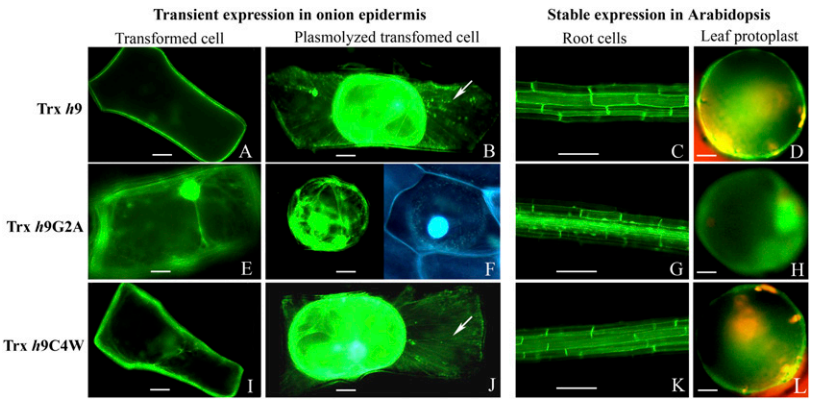

Fig. 3. Subcellular localization of wild-type and mutated Trx *h*9 in onion epidermal and transgenic *Arabidopsis* cells using GFP tagging. (*A*–*D*) Trx *h*9. (*E*–*H*) Trx *h*9G2A. (*I*–*L*) Trx *h*9C4W. *A* and *B*, *E* and *F*, and *I* and *J* show transient expression of wild-type and mutated Trx h9-GFP in onion epidermal cells. *C* and *D*, *G* and *H*, and *K* and *L* show stable expression patterns of wild-type and mutated Trx *h*9-GFP in *Arabidopsis*. *A*, *E*, and *I* are unplasmolyzed transformed epidermal cells; *B*, *F*, and *J* are plasmolyzed, transformed epidermal cells. *C*, *G*, and *K* are stably transformed root cells; *D*, *H*, and *L*, are stably transformed mesophyll protoplasts. Image in *F* viewed for GFP (*Left*) and DAPI (*Right*). [Scale bars, 50 μm (*C*, *G*, and *K*); 10 μm (remainder).] In *B* and *J*, arrows point to Hechtian strands.

3 *K* and *L*). Localization results led to the conclusion that association of Trx *h*9 with the plasma membrane is possibly linked to *N*-myristoylation modification at Gly^2 but is independent of Cys^4.

Trx *h*9 Can Move from Cell to Cell. That Trx *h*9 is membrane-anchored and has the potential for palmitoylation suggested a unique function relative to its Trx counterparts. As palmitoylation has been associated with protein movement in animal cells, we sought evidence of a related function in plants (18, 20). We therefore tested the possible movement of Trx *h*9 using the *Arabidopsis* tissue-specific promoter SCARECROW (pSCR), which directs downstream gene expression specifically in the single endodermal cell layer of the root (21). Before examining expression of Trx h9, we confirmed promoter specificity with two other Trxs (Trx *h*2 and Trx *p*), their full-length protein-coding sequences fused to GFP, pSCR::Trx *h*2-GFP and pSCR::Trx *p*-GFP, respectively. Confocal imaging confirmed that both Trx-GFP fusions (pSCR::Trx *h*2-GFP and pSCR::Trx *p*-GFP) showed the expected expression in the single endodermal layer of the root tip (Fig. 4 *A*, *B* and *C*, *D*). By contrast, in plants transformed with pSCR::Trx *h*9-GFP, GFP was seen throughout the root (Fig. 4 *E* and *F*). These results suggest that, unlike other Trxs examined to date, Trx *h*9 can move from cell to cell, that is, migrate from its original expression site in endodermal cells to other cell layers of the root (Fig. 4 *E* and *F*). This type of movement differs from that described for truncated human Trx (Trx80) and NaTrx*h* from *Nicotiana alata* that cross the cell boundary during secretion (22, 23). It is also different from that for 13-kDa rice cytosolic *h*-type Trx, RPP13-1, that moves from companion cells through plasmodesmata into adjacent sieve elements in mature phloem (24). It is noted that the apparent absence of Trx *h*9 movement in isolated epidermal onion tissue described above suggests the requirement for a condition provided only by the living plant.

Trx *h*9 Movement Requires Both Gly^2 and Cys^4. As observed for its membrane localization (Fig. 3 *E* and *F*), Trx *h*9 movement was abolished by replacing Gly^2 with alanine (Fig. 4 *G* and *H*). However, unlike localization, which was not altered by mutagenizing Cys^4 (Fig. 3 *I*–*L*), movement of Trx *h*9 was also abolished by converting Cys^4 to tryptophan (Fig. 4 *I* and *J*). Palmitoylation occurs in membranes, and thus cytosolic proteins must interact with membranes to be palmitoylated (17, 18). Gly^2 may, therefore, be required for membrane localization of Trx *h*9 and for subsequent palmitoylation of Cys^4. Palmitoylated proteins, which favor specific protein-protein interactions, modulate the activity of signaling cascades (18). Although Cys^4 was not required for membrane localization of Trx *h*9, the dynamically palmitoylated Cys^4 may enhance its membrane association and facilitate its movement by regulating its activities and interactive properties. Taken together, these results suggest that the two conserved amino acids in the N-terminal extension of Trx *h*9 are essential for its unusual properties: Gly^2 for membrane anchoring and both Gly^2 and Cys^4 for mobility. Interestingly, Cys^4 of Trx h9 seems to be the target not only for movement but also for its reduction by glutaredoxin, as suggested by results obtained with the ortholog from poplar (19). However, mechanisms as to how these two reactions involving the same thiol group are regulated with respect to each other remain to be determined. Mutation analysis in terms of movement and palmitoylation of Cys^{57} in the catalytic site of Trx *h*9 would provide insight into this question.

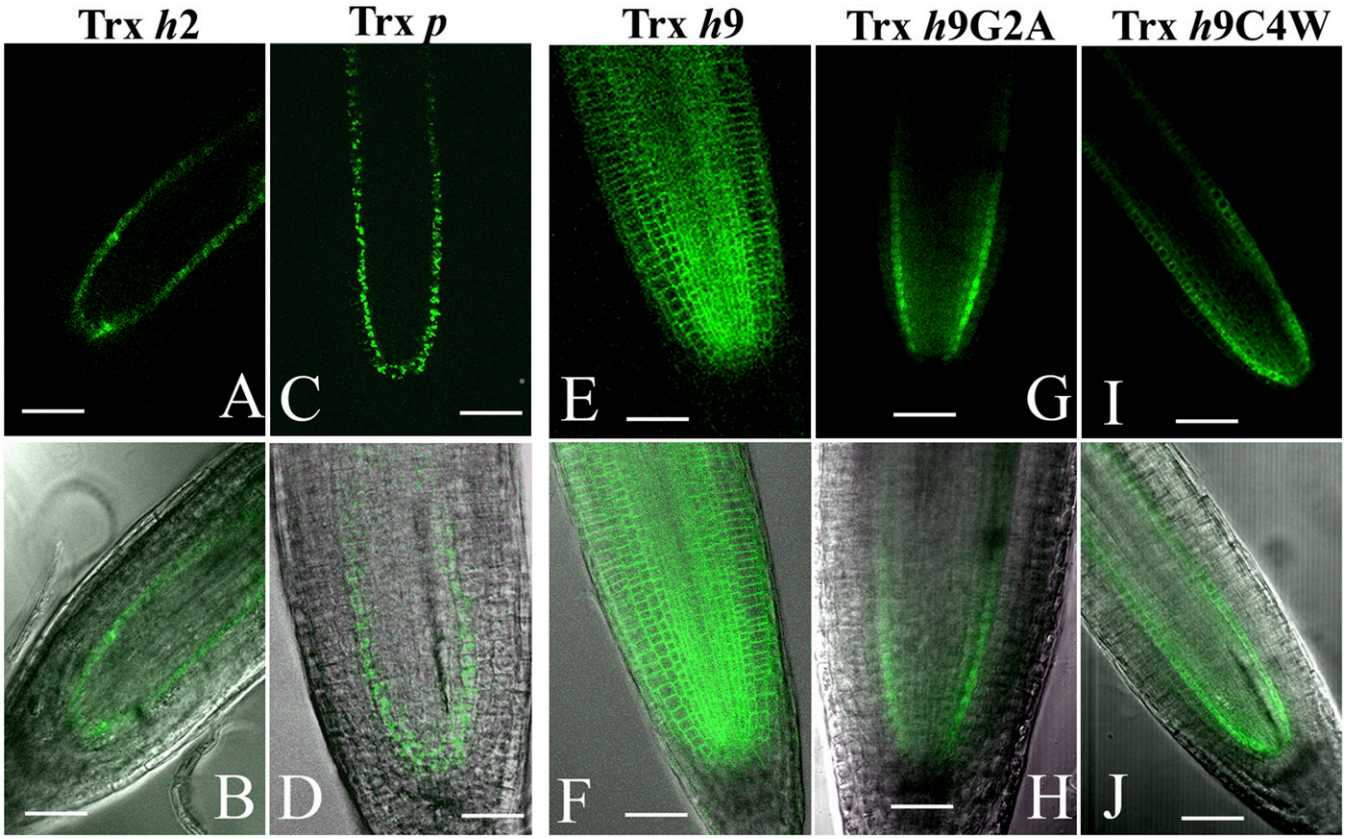

Fig. 4. Movement analysis of Trx *h*9 protein in root tips of 7-day-old *Arabidopsis* (Col-0) seedlings using *Arabidopsis SCARECROW* promoter (pSCR) and GFP tag. (*A* and *B*) Trx *h*2 (At5g39950). (*C* and *D*) Trx *p* (At3G06730). (*E* and *F*) Trx *h*9. (*G* and *H*) Trx *h*9G2A. (*I* and *J*) Trx *h*9C4W. (Scale bars, 50 μm.)

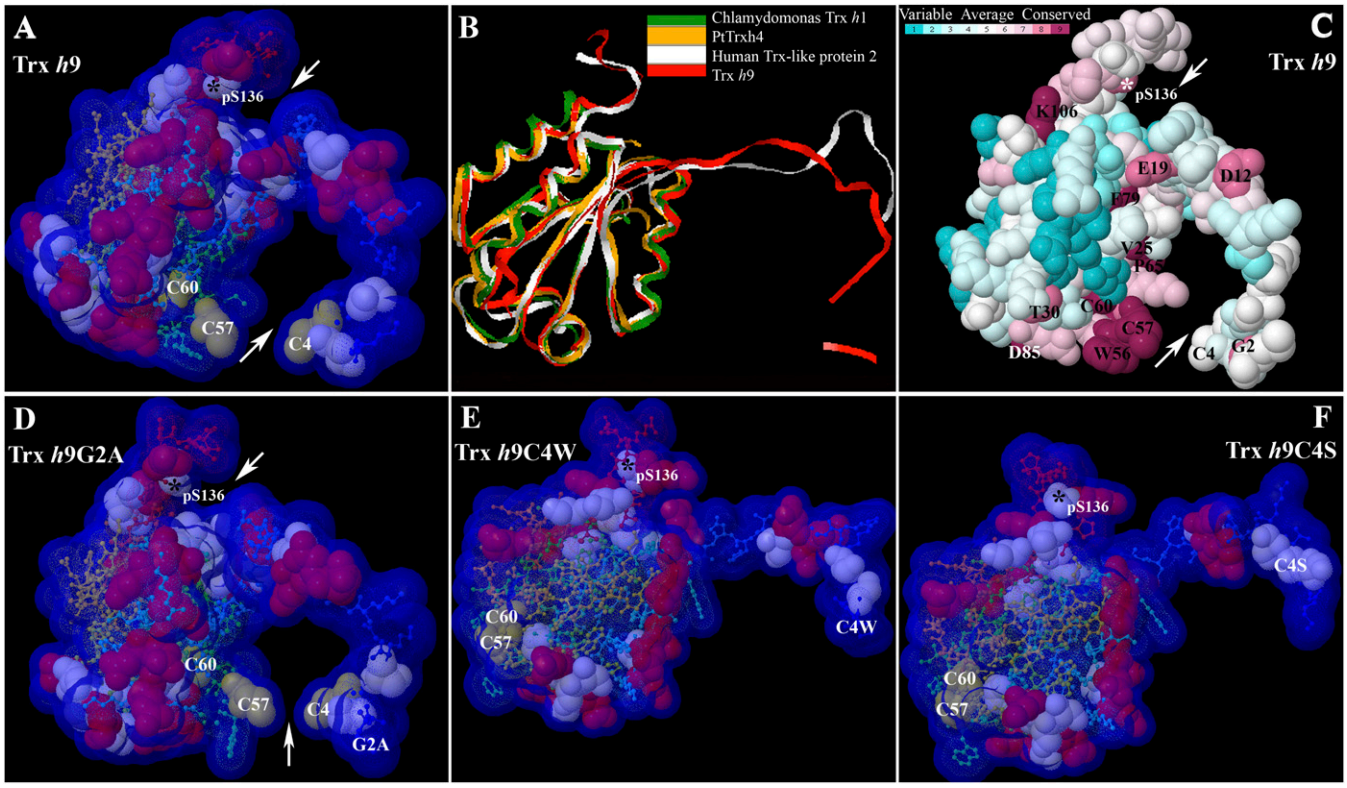

Fig. 5. Three-dimensional models and conserved residue prediction for Trx *h*9. (*A*) Three-dimensional model of Trx *h*9. (*B*) Superimposition of 3D model of Trx *h*9 (red) and the top three templates of Trx *h*9: *C. reinhardtii* Trx *h*1 (green; PDB ID code 1ep7A); poplar PtTrx*h*4 (yellow; PDB ID code 3d21); and human Trx-like protein 2 (white; PDB ID code 2diyA), using 3d-SS (3-Dimensional Structural Superposition) service. (*C*) Conserved residue analysis of Trx *h*9. Residue conservation from variable to conserved is shown in green to dark red, respectively. (*D–F*) Three-dimensional model of Trx *h*9G2A, Trx h9C4W, and Trx h9C4S, respectively. Arrows point to potential docking sites of Trx h9 in *A*, *C*, and *D*. Cys, Ser, and positively charged residues are shown in off-yellow, light blue, and red, respectively, as 100% of van der Waals. The remainder of residues from N to C terminus are shown in blue to red as 20% of van der Waals in *A* and *D*, and *E* and *F*. All atoms are coupled with Solvent-Accessible Surface (VDW + 1.4 Å) in *A* and *D–F*. Asterisks indicate phosphorylated Ser at position 136 (pS136) at the C terminus of Trx *h*9. Conserved amino acids with single-letter abbreviations are indicated at their numbered position in *C*.

Trx *h*9 May Dock via Interaction of N-Terminal Cys^4 with Catalytic Cys^{57}. Sequence analysis reveals that Trx *h*9 has 70% identity with a Trx from poplar (PtTrx*h*4), the 3D structure of which has been determined (19). Using PtTrx *h*4 and other close homologs as templates for comparative modeling, we determined a predicted 3D structure for Trx *h*9 by applying I-TASSER simulation (25) (Fig. 5*A*) that matched nearly perfectly with Zits templates (Fig. 5*B*) (*SI Materials and Methods*). Analysis of its structure revealed that, as discussed by Koh et al. (19), the N-terminal extension appears to act like an arm appended to the main body of Trx *h*9 with the potential to be a protein docking site (binding pocket)—through possible interaction of the N-terminal Cys (Cys^4) with Cys^{57} in the classical catalytic site (C^{57}GPC^{60}) (Fig. 5*A*).This docking site could confer specific binding properties to Trx *h*9 in its interaction with other proteins in a manner possibly modulated by palmitoylation of Cys^4. In addition, the C terminus of Trx *h*9 could form a smaller binding pocket in which Ser^{136} is located at the inside surface. The reported phosphorylation of Ser^{136} in response to sucrose (26) could alter binding properties of the pocket. An analysis of the evolutionary conservation of its surface amino acids using ConSurf (http://consurf.tau.ac.il) provided further evidence that the N-terminal extension of Trx *h*9, especially Gly^2, appears to have functional significance (Fig. 5*C*).

To assess the contribution of the conserved N-terminal Gly^2 and Cys^4 to structure, we constructed 3D models for three Trx *h*9 mutants—Trx h9G2A, Trx *h*9C4W, and Trx *h*9C4S—using the I-TASSER method. Gly^2 was replaced by Ala in Trx *h*9G2A and Cys^4 by both Trp in Trx *h*9C4W and Ser in Trx *h*9C4S. Mutation of Gly^2 had relatively little effect on the 3D structure; the N-terminal extension appeared still to be able to form a binding pocket (Fig. 5*D*). However, replacing Cys^4 with either Trp or Ser dramatically altered the structure (Fig. 5 *E* and *F*). The N-terminal extension appeared to move away from the main body of the molecule, seemingly leading to loss of the binding pocket and the ability of Cys^4 to interact with catalytic Cys^{57}.

Grx, Not NTR, Fits in the Potential Binding Pocket of Trx *h*9. Computational docking methods used to predict protein-protein interactions can help define parameters valuable to understanding biochemical mechanisms. When analyzed in this manner, Trx *h*9 appeared not to interact with NADP-thioredoxin reductase (NTR), like other *h*-type Trxs such as *h*1 (Fig. S6 *A* vs. *B*). Rather, its predicted structure indicated that it might be preferentially reduced by the GSH/Grx system, as for the poplar ortholog of Trx *h*9, PtTrx*h*4 (6) (Fig. S6 *D* and *E*) in an interaction dependent on Cys^4 but not Gly^2 (Fig. S6 *H* and *I* and *F* and *G* and *SI Text*).

Conclusion

An *h*-type Trx *h*9, was found to bind to the plasma membrane despite lacking a transmembrane domain. Experiments with the SCARECROW promoter revealed that Trx *h*9 was mobile, with the capability to move from cell to cell. Two amino acids in its N-terminal extension appeared to be responsible for these unique properties. Gly^2 was required for association with the plasma

membrane (possibly for myristoylation), and both Gly^2 and Cys^4 were essential for mobility (the latter seemingly for structure and palmitoylation). A modeling analysis indicated that Trx *h*9 is preferably reduced by GSH and Grx, similar to its poplar ortholog, rather than by NTR, as described for other *h*-type Trxs. A T-DNA insertion mutation revealed that Trx *h*9 was required for growth and development. Trx *h*9 thus appears to resemble Trx *h*3 (27) in bridging the Grx/Trx interface in relaying information to maintain cellular redox balance. It seems possible that Trx *h*9 may be required for redox signaling. Finally, control experiments uncovered a Trx *h* (*h*2) residing in mitochondria and a plastid Trx (Trx *p*) previously identified described as cytosolic (8). It will be of interest to see how Trx *h*9 contributes to plant growth and development, including the germination of seeds, and how Trx *h*2 and Trx *p* function in their respective organelles.

Materials and Methods

Expression Analysis and Screening for T-DNA Insertion Mutants. Expression was analyzed by quantitative RT-PCR (*SI Materials and Methods*). Lines with a putative T-DNA insertion in *Trx h*9, Salk_086660, or in *Trx p*, Salk_028162, were obtained from the *Arabidopsis* Biological Resource Center. T-DNA insertions and expression of the relevant genes in the Salk lines were screened by PCR sequencing and RT-PCR, respectively (*SI Materials and Methods*).

Constructs. Full-length coding sequence of the *Trx*s and an ~2.6-kb fragment immediately upstream of the *SCARECROW* coding sequence were amplified by PCR from genomic DNA of *Arabidopsis* Col-0 plants using appropriate primers (Table S2). EcoRI and BamHI cloning sites and mutated sequences were incorporated into the 5′ forward primers (Table S2, indicated by underline). PCR products from the *Trx*s were cloned into pEZS-NL vector at the EcoRI and BamHI sites for transient transformation. For stable transformation, a NotI fragment, with each cloned *Trx* gene linked to the 35S promoter and *OCS 3′*, was removed from pEZS-NL and inserted into binary vector pART27. The ~2.6-kb fragment from *Scarecrow* (21) replaced the 35S promoter in pEZS-NL at NotI and EcoRI sites (Table S2). The NotI fragment with pSCR promoter::Trx-GFP was transferred to pART27.

Transient Expression Assays Using Particle Bombardment of Isolated Onion Epidermal Cell Layer. Plasmids with the 35S::Trx-GFP fusion were individually bombarded into onion epidermal cells (28), which were examined for GFP (see below). After 20–24 h postparticle bombardment, onion epidermal cells were stained with DAPI (29). Cells were plasmolyzed by incubating 10 min in each of 0.25, 0.50, and 0.75 M sucrose.

Plant Transformation, Selection, Protoplast Generation, and Fluorescence Visualization. Trx constructs in pART27 were introduced into *Agrobacterium tumefaciens* GV3101, using the freeze–thaw method (30), and the transformed *Agrobacterium* was then introduced into *Arabidopsis* via the floral-dip method (31). T_1 plants were selected on MS medium containing 50 μg/L kanamycin. *Arabidopsis* plants were grown in soil in the greenhouse or on MS medium with 1.0% sucrose (16 h light/8 h dark cycle, 23 °C). Protoplasts were generated from transgenic leaves by treating 30 min with 1.0% cellulase, 0.5% pectinase, 1.0 mg/mL BSA, 0.048% PVP, 0.5 M sucrose, 1.0 mM $CaCl_2$ (pH 5.5), and used immediately to examine for GFP. Fluorescence was visualized using a Leica DM LB fluorescence microscope or a Zeiss LSM 510 confocal microscope with 488 nm/530 nm excitation/emission light for GFP, 364/470 for DAPI, and 543/576 for MitoTracker orange.

Prediction of 3D Structure of Trx *h*9. The three-dimensional structure of Trx *h*9 was predicted using I-TASSER (threading/assembly/refinement), that is, Zhang service (25), available at http://zhang.bioinformatics.ku.edu/I-TASSER. Superimposition analysis of the 3D models of Trx *h*9 and its templates [human Trx-like protein 2 (PDB ID code 2diyA), PtTrxh4 (PDB ID code 3d21A), and Trx *h*1 from *Chlamydomonas reinhardtii* (PDB ID code 1ep7A)] was done using 3-Dimensional Structural Superposition (3d-SS) service (http://cluster.physics.iisc.ernet.in/3dss/severalinput.html) (32). Conserved amino acids at the protein surface were determined using ConSurf (33) (http://consurf.tau.ac.il/overview.html).

ACKNOWLEDGMENTS. The authors thank Drs. S. Ruzin and D. Schichnes of the UCB Biological Imaging Facility for assistance, S. Cutler and D. Ehrhardt for pEZS-NL, Catherine Lie, SuFey Ong, and Khanh Nguyen for laboratory assistance, and Z. Li for chlorophyll analysis. L.M. was partially supported by the Agricultural and Environmental Chemistry Graduate Program, P.G.L. by the US Department of Agriculture Cooperative Extension, and B.B.B. by the Agricultural Experiment Station, University of California.

1. Foyer CH, Noctor G (2005) Redox homeostasis and antioxidant signaling: A metabolic interface between stress perception and physiological responses. *Plant Cell* 17: 1866–1875.
2. Fujino G, Noguchi T, Takeda K, Ichijo H (2006) Thioredoxin and protein kinases in redox signaling. *Semin Cancer Biol* 16:427–435.
3. Sweat TA, Wolpert TJ (2007) Thioredoxin *h*5 is required for victorin sensitivity mediated by a CC-NBS-LRR gene in *Arabidopsis*. *Plant Cell* 19:673–687.
4. Tada Y, et al. (2008) Plant immunity requires conformational changes [corrected] of NPR1 via S-nitrosylation and thioredoxins. *Science* 321:952–956.
5. Li YC, et al. (2009) The level of expression of thioredoxin is linked to fundamental properties and applications of wheat seeds. *Mol Plant* 2:430–441.
6. Gelhaye E, Rouhier N, Jacquot JP (2003) Evidence for a subgroup of thioredoxin *h* that requires GSH/Grx for its reduction. *FEBS Lett* 555:443–448.
7. Reichheld J-P, Mestres-Ortega D, Laloi C, Meyer Y (2002) The multigenic family of thioredoxin *h* in *Arabidopsis thaliana*: Specific expression and stress response. *Plant Physiol Biochem* 40:685–690.
8. Rivas S, et al. (2004) CITRX thioredoxin interacts with the tomato Cf-9 resistance protein and negatively regulates defence. *EMBO J* 23:2156–2165.
9. Lichtenthaler HK (1969) Die Plastoglobuli von Spinat, ihre Grösse, Isolierung und Lipochinonzusammensetzung. *Protoplasma* 68:65–77.
10. Marcus F, et al. (1991) Plant thioredoxin *h*: An animal-like thioredoxin occurring in multiple cell compartments. *Arch Biochem Biophys* 287:195–198.
11. Gelhaye E, et al. (2004) A specific form of thioredoxin *h* occurs in plant mitochondria and regulates the alternative oxidase. *Proc Natl Acad Sci USA* 101:14545–14550.
12. Lang-Pauluzzi I, Gunning BES (2000) A plasmolytic cycle: The fate of cytoskeletal elements. *Protoplasma* 212:174–185.
13. Buchanan BB, Balmer Y (2005) Redox regulation: A broadening horizon. *Annu Rev Plant Biol* 56:187–220.
14. Gelhaye E, Rouhier N, Navrot N, Jacquot JP (2005) The plant thioredoxin system. *Cell Mol Life Sci* 62:24–35.
15. Casey PJ (1995) Protein lipidation in cell signaling. *Science* 268:221–225.
16. Maurer-Stroh S, Eisenhaber B, Eisenhaber F (2002) N-terminal *N*-myristoylation of proteins: Refinement of the sequence motif and its taxon-specific differences. *J Mol Biol* 317:523–540.
17. Resh MD (1999) Fatty acylation of proteins: New insights into membrane targeting of myristoylated and palmitoylated proteins. *Biochim Biophys Acta* 1451:1–16.
18. Smotrys JE, Linder ME (2004) Palmitoylation of intracellular signaling proteins: Regulation and function. *Annu Rev Biochem* 73:559–587.
19. Koh CS, et al. (2008) An atypical catalytic mechanism involving three cysteines of thioredoxin. *J Biol Chem* 283:23062–23072.
20. Zhou B, Liu L, Reddivari M, Zhang XA (2004) The palmitoylation of metastasis suppressor KAI1/CD82 is important for its motility- and invasiveness-inhibitory activity. *Cancer Res* 64:7455–7463.
21. Malamy JE, Benfey PN (1997) Analysis of *SCARECROW* expression using a rapid system for assessing transgene expression in *Arabidopsis* roots. *Plant J* 12:957–963.
22. Juárez-Díaz JA, et al. (2006) A novel thioredoxin *h* is secreted in *Nicotiana alata* and reduces S-RNase in vitro. *J Biol Chem* 281:3418–3424.
23. Pekkari K, et al. (2003) Truncated thioredoxin (Trx80) exerts unique mitogenic cytokine effects via a mechanism independent of thiol oxido-reductase activity. *FEBS Lett* 539:143–148.
24. Ishiwatari Y, et al. (1998) Rice phloem thioredoxin *h* has the capacity to mediate its own cell-to-cell transport through plasmodesmata. *Planta* 205:12–22.
25. Zhang Y (2008) I-TASSER server for protein 3D structure prediction. *BMC Bioinformatics* 9:40.
26. Niittylä T, Fuglsang AT, Palmgren MG, Frommer WB, Schulze WX (2007) Temporal analysis of sucrose-induced phosphorylation changes in plasma membrane proteins of *Arabidopsis*. *Mol Cell Proteomics* 6:1711–1726.
27. Reichheld J-P, et al. (2007) Inactivation of thioredoxin reductases reveals a complex interplay between thioredoxin and glutathione pathways in *Arabidopsis* development. *Plant Cell* 19:1851–1865.
28. Scott A, Wyatt S, Tsou PL, Robertson D, Allen NS (1999) Model system for plant cell biology: GFP imaging in living onion epidermal cells. *Biotechniques* 26:1125–1132, 1128–1132.
29. Khar A, Mitchison JM (1989) Observations on ultracentrifuging wild-type and mutant (*cdc2.33*) cells of *Schizosaccharomyces pombe*. *J Cell Sci* 92:345–348.
30. Höfgen R, Willmitzer L (1988) Storage of competent cells for *Agrobacterium* transformation. *Nucleic Acids Res* 16:9877.
31. Clough SJ, Bent AF (1998) Floral dip: A simplified method for *Agrobacterium*-mediated transformation of *Arabidopsis thaliana*. *Plant J* 16:735–743.
32. Russell RB, Breed J, Barton GJ (1992) Conservation analysis and secondary structure prediction of the SH2 family of phosphotyrosine binding domains. *FEBS Lett* 304: 15–20.
33. Landau M, et al. (2005) ConSurf: The projection of evolutionary conservation scores of residues on protein structures. *Nucleic Acids Res* 33 (Web Server issue):W299–W302.